Published in final edited form as:
J Mol Cell Cardiol. 2013 September ; 62: 51–57. doi:10.1016/j.yjmcc.2013.05.001.

The connection between inner membrane topology and mitochondrial function

Carmen A. Mannella[a,*], **W. Jonathan Lederer**[b], and **M. Saleet Jafri**[c]

[a]Wadsworth Center, New York State Department of Health, Empire State Plaza, Box 509, Albany, NY 12201-0509, USA

[b]Center for Biomedical Engineering and Technology, University of Maryland School of Medicine, Baltimore, MD 21201, USA

[c]School of Systems Biology and Department of Molecular Neuroscience, George Mason University, Fairfax, VA 22030, USA

Abstract

The mitochondrial inner membrane has a complex and dynamic structure that plays an important role in the function of this organelle. The internal compartments called cristae are created by processes that are just beginning to be understood. Crista size and morphology influence the internal diffusion of solutes and the surface area of the inner membrane, which is home to critical membrane proteins including ATP synthase and electron transport chain complexes; metabolite and ion transporters including the adenine nucleotide translocase, the calcium uniporter (MCU), and the sodium/calcium exchanger (NCLX); and many more. Here we provide a brief overview of what is known about crista structure and formation, and discuss mitochondrial function in the context of that structure. We also suggest that mathematical modeling of mitochondria that incorporates accurate information about the organelle's internal architecture can lead to a better understanding of its diverse functions. This article is part of a Special Issue entitled 'Calcium Signalling in Heart'.

1. Introduction

As cellular organelles go, mitochondria are arguably the most structurally and functionally diverse across species and across tissues in the same species. In mammals, the mitochondrial proteome contains on the order of 1100 proteins, not counting a wide array of splicing and post-translational variants [1]. The proteins associated with key processes that mitochondria in all tissues have in common, such as oxidative phosphorylation and organelle biogenesis and dynamics, comprise only about one-third of the proteome. The mitochondrial proteome of any two tissues typically varies by 20–30%, reflecting the specialized metabolic and signaling pathways within mitochondria of different cell types. While they share a common

*Corresponding author: Tel.: +1 518 474 2462., carmen@wadsworth.org (C.A. Mannella).

Supplementary data to this article can be found online at http://dx.doi.org/10.1016/j.yjmcc.2013.05.001.

Conflict of interest
None declared.

bacterial ancestor, mitochondria are finely tuned to the physiology of the cells into which they have integrated over hundreds of millions of years of evolution.

Thanks to the pioneering work of Palade, Sjostrand and others, the ultrastructural diversity of mitochondria was appreciated long before the functional differences that underlie it (e.g. [2]). Within the diversity, a common organelle design was readily discerned in electron micrographs: nested outer and inner boundary membranes surrounding a dense “matrix”. The mitochondrial inner membrane seemed to fold inwards to form what Palade called cristae (crests), the density of which varied roughly in proportion to the energy demands of the tissues. Once it was established in the 1960s that the inner membrane was the site of the respiratory chain and oxidative phosphorylation, interest grew in the relevance of the membrane’s structure to bioenergetic processes. This interest was heightened by Hackenbrock’s discovery of correlations between particular respiratory states and inner membrane morphologies (so called *orthodox* and *condensed* states) in isolated mitochondria [3]. The emergence and eventual acceptance of Mitchell’s chemiosmotic hypothesis [4] gave rise to discussions that still persist about possible micro-compartmentation of protons and delocalized vs. local proton gradients across the inner membrane during energy transduction [5].

The terms “folds” and “invaginations” are often used interchangeably to describe cristae, but the terms are not synonymous. The former suggests random, passive adjustments of a flexible membrane to osmotic or other forces. The latter term implies a membrane domain with complex topology and origins. We now realize that cristae are, in fact, specialized nano-scale structures that influence mitochondrial function and, in turn, are regulated by molecular mechanisms we are only beginning to comprehend.

2. The link between inner membrane topology and function

An important step in the evolution of electron microscopy was the convergence of developments in hardware and software in the 1980s that made high resolution three dimensional reconstructions practical. The mitochondrion’s structural complexity and diversity, combined with spiraling interest among biologists in its multiple cellular functions, made the organelle a poster child for the technique of electron tomography [6–9]. As shown in Fig. 1, the cristae in cardiac muscle mitochondria (as in almost all mitochondria) are not merely random folds in the inner membrane. Rather, they are distinct, pleomorphic compartments, a mixture of tubular structures and larger, usually lamellar cisternae. These “invaginations” are connected to the boundary region of the inner membrane at narrow circular or slot-like “junctions”, with a bore as small as 10 nm (determined from tomograms of intact, frozen hydrated mitochondria [10]). The junctions are robust, energetically favored structures, reversibly reforming within several minutes after extreme osmotic swelling and recontraction of yeast mitochondria [10].

The common design element of crista junctions (first described by Daems and Wisse [11]) has profound implications for regulation of mitochondrial processes involving internal diffusion of ions, metabolites and proteins. For example, Mannella et al. speculated that crista junctions might serve to compartmentalize protons involved in chemiosmosis [6,7,12],

a possibility that has been expanded upon by others [5,13]. Also, computer simulations demonstrated that the ADP concentration in large intracristal compartments connected by narrow junctions to the inner boundary membrane could drop below the K_m of the adenine nucleotide translocator, resulting in reduced local ATP generation [10]. These simulations were done using a crista from a *condensed* (matrix contracted) liver mitochondrion, typical for respiratory state III (high [ADP]) [3]. When [ADP] is low (state IV), mitochondria switch to the *orthodox* (matrix expanded) conformation in which cristae are smaller. This structural change would be expected to reduce the diffusional bottleneck for ADP, which is more important when ADP is limiting than when it is in excess [15]. Additional modeling of the diffusion of ions and metabolites inside muscle mitochondria is presented below. Interestingly, for a 2D model simulating tubular cristae (common in *orthodox* mitochondria), there is no appreciable intracristal ADP gradient under similar conditions (Fig. 5).

Thus, changes in mitochondrial inner membrane topology are expected to influence mitochondrial bioenergetic processes in vivo. It follows that inner membrane topology could be a parameter regulated by the cell to optimize mitochondrial function [14–16]. Proof of this hypothesis requires uncovering the molecular players and signaling pathways involved in regulation of crista structure and organization.

There is evidence that typical crista structures, including the reversible *condensed–orthodox* transition, represent a dynamic balance between fusion and fission of tubular cristae, and that aberrant crista morphologies (observed in some physiological and pathological states) result from an imbalance in the processes [14,15]. Tomograms of frozen hydrated mitochondria give a strong impression that larger cristae are formed by fusion of tubular and perhaps vesicular cristae ([10], Fig. 2).

A good example of the linkage of inner membrane dynamics to mitochondrial function is the remodeling of the inner membrane associated with the intrinsic apoptotic pathway. Korsmeyer and co-workers showed that addition of truncated Bid (tBid, a cellular trigger for intrinsic apoptosis) to isolated liver mitochondria causes a rapid reversal of crista curvature, accompanied by apparent fusion of cristae and widening of crista junctions into large slots (Fig. 2) [17]. This dramatic topological change correlates with enhanced internal mobilization and release from mitochondria of cytochrome *c*, needed to activate cytosolic caspases. Frey, Perkins and colleagues showed that induction of apoptosis in HeLa cells also results in a widening of crista junctions, which progresses to create septa that divide the inner membrane into individual vesicular domains [18], likely a precursor to the fission of mitochondria observed in later stages of apoptosis.[1]

[1]It was recently reported that mitochondria in the flattened leading edges of frozen-hydrated human endothelial cells contain mostly septum-like cristae with wide openings [19]. Also, frozen-hydrated fungal mitochondria, deliberately flattened by surface tension, were reported to have primarily wide (200 nm) slot-shaped junctions [20] We have found some variability in the size of crista junctions in frozen hydrated, unflattened, isolated liver and fungal mitochondria ([10] and Mannella, Hsieh, Marko, unpublished) but the openings generally fall in the 10–50 nm range. Importantly, small crista junctions are also found in mitochondria in frozen hydrated sections of liver [21]. It is possible that flattening of mitochondria (isolated or inside cells) prior to freezing induces widening of crista junctions.

3. Molecular determinants of inner membrane topology

There is considerable evidence to suggest that the tBid induced change in inner membrane topology (Fig. 2) is related to molecular reorganizations involving cardiolipin and the adenine nucleotide translocator, the most prevalent inner membrane protein (reviewed in [15,16]). Whether the associated enhancement of cytochrome *c* efflux is due to changes in internal diffusion (e.g., elimination of narrow crista junctions that may at times be closed or pinched off) or to changes in binding of cytochrome *c* to the inner membrane is not yet known. There is strong evidence that the changes in inner membrane topology that occur during apoptosis also involve the dynamin-like protein Opa1 (Mgm1 in yeast). Opa1 was originally discovered as a required component of the mitochondrial fusion machinery, and later implicated in maintaining normal crista morphology [22–24]. The Scorrano lab has postulated a kind of gating mechanism involving oligomerization of two forms of Opa1, occurring on the outer and inner mitochondrial membranes. Caspase 8 cleaved BID (a precursor to fully truncated BID) disrupts Opa1 oligomers and widens the junction openings [24]. Opa1 defects in humans are associated with a serious neuropathy, autosomal dominant optic atrophy, and skin fibroblasts from these patients have distorted crista structure [25]. Functional mutants of Opa1 in *Caenorhabditis elegans* have a slow metabolism and their mitochondria contain numerous detached cristae in the matrix [26]. Just as widening crista junctions correlates with increased internal diffusion rates [17], eliminating communication of cristae with the intermembrane space would be expected to drastically diminish mitochondrial energy metabolism. A thorough analysis is needed to determine the extent to which the bioenergetic deficits in dominant optic atrophy are attributable to disruption of normal crista topology.

Research in the past decade has uncovered several other molecular determinants of crista morphology, in particular ATP synthase (reviewed in [16,27]). The first clues that linear arrays of ATP synthase dimers were involved in tubularization of the inner membrane were provided by scanning electron microscopy of deep-etched *Paramecium* mitochondria [28]. Later, yeast, bearing mutations in subunits of ATP synthase involved in oligomerization of the complex, were found to lack normal crista formation [29]. Supporting evidence for the role of ATP synthase dimers in bending the mitochondrial inner membrane came first from single particle analysis of isolated dimers [30,31] and more recently from cryo-electron tomography of yeast inner membrane fragments [13,32]. Assuming cristae are proton traps (as mentioned earlier), it has been speculated that locating ATP synthase complexes (proton sinks) at the narrow openings of the cristae could be a self-organizing feature that optimizes ATP generation [13].

Another concept about regulation of mitochondrial inner membrane organization involves interactions between the inner and outer membranes. Electron micrographs of conventionally fixed and stained mitochondria show numerous points of close proximity between outer and inner membranes, termed “contact sites” [3]. However, electron tomograms of native (unfixed, unstained) frozen-hydrated mammalian mitochondria (isolated and in tissue sections [10,21]) provide better resolution and indicate that points of actual contact between the two membranes are rare. Instead, numerous ~10 nm “bridging particles” can be seen in the intermembrane space that, it has been postulated, likely mediate

inner–outer membrane interactions and the numerous physiological processes attributed to these specialized regions [10,14].

In fact, a protein complex recently has been identified that stabilizes mitochondrial inner membrane organization by attaching to proteins on the outer and inner membranes. When expression of a conserved protein called mitofilin is knocked down in mammalian cells, onion-like membrane structures form inside the mitochondria, suggesting mitofilin is involved in generating or stabilizing normal crista structure [33]. Recently mitofilin (Fcj1 in yeast) was identified as part of a “contact site” protein complex implicated in formation of crista junctions in yeast mitochondria [34,35]. Members of this complex interact with both inner and outer membrane proteins, including ATP synthase dimers [34]. The functions of this large intermembrane “scaffold” complex and its individual components – several of which, like Fjc1, are essential for maintaining normal crista integrity – are under active investigation [36,37].

Finally, any discussion of factors influencing inner membrane topology should include mention of the respiratory “supercomplexes” (e.g. [38,39]). Respiratory chain proteins are more prominent in cristae than in the peripheral regions of the mitochondrial inner membrane (e.g. [40,41] and the complexes they comprise tend to form megadalton-size assemblies (supercomplexes) with specific stoichiometries. While there is scant structural information about the supercomplexes, it would not be surprising if either (a) they segregated to particular inner membrane domains (such as planar cristae), or (b) played a more active role, analogous to ATP synthase dimer ribbons, in influencing inner membrane curvature.

4. Mathematical models of cristae and mitochondrial function

To explore the role of crista morphology in mitochondrial function, mathematical models add an important tool for examining specific hypotheses [10]. In this early phase of our exploration, we are using simplified versions of realistic crista structures and assuming uniform distribution of components to model internal diffusional processes, rates of transport, and physiological and pathophysiological features. Fig. 3 shows the densely packed cristae that take up approximately 50% of the volume in rat cardiac mitochondria [42,43]. The scanning electron micrographs reveal two extremes in crista morphology: lamellar cristae that predominate in subsarcolemma regions (Fig. 3A) and tubular cristae that are most common in interfibrillar mitochondria (Fig. 3B) [37]. Whether this structural heterogeneity among mitochondria within the same tissue has a functional rationale is currently unknown, but modeling of important physiological processes for the two extremes in crista topology (tubular vs. lamellar) could provide valuable insights.

The diagram of Fig. 4 shows an idealized cardiac mitochondrion with almost 300 regularly packed “tubular” cristae, each with a square 20 × 20 nm cross-section and a length of 240 nm. The inner membrane surface area is about 3 times the surface area of the outer membrane and the matrix volume fraction is about half of the volume contained within the outer membrane, an organization that may apply to typical intermyofibrillar rat mitochondria (Chikando et al. [44]).

A simplified 2D simulation was carried out to reveal the nature of solute gradients likely to exist in simple tubular cristae of a cardiac mitochondrion like that in Fig. 4. The steady-state concentration gradients that develop along the length of two cristae for $[H^+]_c$, $[Ca^{2+}]_c$, $[ATP]_c$, $[ADP]_C$, $[Phosphate]_c$ and $[Na^+]_c$ are shown in Fig. 5 (panels A–F, respectively). Because such models can take into account all constrained elements (e.g., ATP synthase, electron transport chain, mitochondrial calcium uniporter (MCU), mitochondrial sodium/calcium exchanger (NCLX), etc.), and can be modified as new information becomes available on crista structure and dynamics, inner membrane protein distribution, and transporter and channel characteristics, these models can test current and future hypotheses. While in its infancy, such multiscale modeling can explore, in parallel, structural and functional information and changes manifest over spatial and temporal scales that span many orders of magnitude (nm to μm, and μs to hours).

The standing concentration gradients inside cristae (like those in Fig. 5) would be expected to vary dramatically during normal cellular activity, such as changes in ATP consumption triggered by metabolic demands, or with alterations associated with disease states. Similarly, normal cyclic activity in muscle would be reflected in time-dependent changes in these gradients. For example, Fig. 6 shows the predicted effect of the cardiac $[Ca^{2+}]_i$ transient on $[Ca^{2+}]_c$ (an animation is provided as Supplemental Material). The systolic (cell-wide) $[Ca^{2+}]_i$ may be as high as 1 μM during the $[Ca^{2+}]_i$ transient and produces the time-dependent gradients down the cristae. Note, also, that there are spatial inhomogeneities of $[Ca^{2+}]_i$ within the cell during the $[Ca^{2+}]_i$ transient that could locally affect Ca^{2+} gradients in the cristae. Importantly, there are transient elevations of microdomain $[Ca^{2+}]$ at both ends of the intermyofibrillar mitochondria (IFM) where local $[Ca^{2+}]_i$ may rise briefly to between 10 and 20 μM [44] because of the proximity of the Ca^{2+} release sites in the cell, the junctional sarcoplasmic reticulum (jSR), to the ends of the mitochondria.

To date there have been many mathematical models that seek to describe mitochondrial function [45–50]. These studies lead the way for future work that will incorporate the growing awareness of the importance of crista spatial organization and dynamics to mitochondrial function.

5. Conclusion

The story that is unfolding on the connection between mitochondrial inner membrane form and function is still in a nascent stage, intriguing but incomplete. There appear to be several mechanisms at work for generating and maintaining normal inner membrane topology, although definition of these processes at the molecular level is far from complete. Furthermore, our understanding of how these mechanisms might be coordinated to remodel the inner membrane in response to cellular signals is fragmentary at best. However, there is plenty of reason for optimism, since the inventiveness of researchers is being matched by steadily advancing technology. The snapshots of frozen-hydrated mitochondria provided by electron tomography are being improved by advances in cryogenic specimen preparation [19,51], and data from super-resolution light microscopy images and single-molecule spectroscopic measurements of membrane events in (preferably) live cells (e.g. [52]). At the same time, theoretical frameworks are being developed that may provide insights into

regulatory processes, such as the role of membrane electrostatics as well as topology in control of intramitochondrial diffusional processes [13] and metabolic regulation of the physical properties of the mitochondrial inner membrane that can affect its remodeling [53]. Combined with improved information about localization and organization of key membrane proteins (e.g. [54,55]), the prospects for more sophisticated and realistic modeling of mitochondrial physiology are excellent. Thus, there is every reason to expect that a more complete picture of the interplay between mitochondrial inner membrane form and function will soon emerge.

Supplementary Material

Refer to Web version on PubMed Central for supplementary material.

Acknowledgments

CAM gratefully recognizes the many colleagues in the fields of electron microscopy and bioenergetics with whom he has collaborated over the years, especially Michael Marko, Chyongere Hsieh, Karolyn Buttle, Yuru Deng, Christian Renken and Joachim Frank. The pioneering technology developments in electron tomography achieved at the Wadsworth Center were made possible by the NIH NCRR biotechnology research center award RR P41 01219. WJL and MSJ acknowledge computational support from H.T. Tuan and G.S.B. Williams and funding from the NIH (R01 AR057348, P01 HL67849, R01 HL105239, R03 TW008425 and R01 HL106059), from the Leducq North American–European Atrial Fibrillation Research Alliance (WJL), and from the European Community's Seventh Framework Programme FP7/2007–2013 under grant agreement no. HEALTH-F2-2009-241526, EUTrigTreat (to WJL). We thank NVIDIA Corporation for donation of GPUs to MSJ.

References

1. Calvo SE, Mootha VK. The mitochondrial proteome and human disease. Annu Rev Genomics Hum Genet. 2010; 11:25–44. [PubMed: 20690818]
2. Munn, EA. The structure of mitochondria. London: Academic Press; 1974.
3. Hackenbrock CR. Ultrastructural bases for metabolically linked mechanical activity in mitochondria. I. Reversible ultrastructural changes with change in metabolic steady state in isolated liver mitochondria. J Cell Biol. 1966; 30:269–97. [PubMed: 5968972]
4. Mitchell P. Keilin's respiratory chain concept and its chemiosmotic consequences. Science. 1979; 206:1148–59. [PubMed: 388618]
5. Williams RJ. Mitochondria and chloroplasts: localized and delocalized bioenergetic transduction. Trends Biochem Sci. 2000; 25:479. [PubMed: 11203381]
6. Mannella CA, Marko M, Penczek P, Barnard D, Frank J. The internal compartmentation of rat-liver mitochondria: tomographic study using the high-voltage transmission electron microscope. Microsc Res Tech. 1994; 27:278–83. [PubMed: 8186446]
7. Mannella CA, Marko M, Buttle K. Reconsidering mitochondrial structure: new views of an old organelle. Trends Biochem Sci. 1997; 22:37–8. [PubMed: 9048477]
8. Perkins G, Renken C, Martone ME, Young SJ, Ellisman M, Frey T. Electron tomography of neuronal mitochondria: three-dimensional structure and organization of cristae and membrane contacts. J Struct Biol. 1997; 119:260–72. [PubMed: 9245766]
9. Frey TG, Mannella CA. The internal structure of mitochondria. Trends Biochem Sci. 2000; 25:319–24. [PubMed: 10871882]
10. Mannella CA, Pfeiffer DR, Bradshaw PC, Moraru II, Slepchenko B, Loew LM, et al. Topology of the mitochondrial inner membrane: dynamics and bioenergetic implications. IUBMB Life. 2001; 52:93–100. [PubMed: 11798041]
11. Daems WT, Wisse E. Shape and attachment of the cristae mitochondriales in mouse hepatic cell mitochondria. J Ultrastruct Res. 1966; 16:123–40. [PubMed: 5956751]

12. Mannella CA. Introduction: our changing views of mitochondria. J Bioenerg Biomembr. 2000; 32:1–4. [PubMed: 11768754]
13. Strauss M, Hofhaus G, Schroder RR, Kuhlbrandt W. Dimer ribbons of ATP synthase shape the inner mitochondrial membrane. EMBO J. 2008; 27:1154–60. [PubMed: 18323778]
14. Mannella CA. The relevance of mitochondrial membrane topology to mitochondrial function. Biochim Biophys Acta. 2006; 1762:140–7. [PubMed: 16054341]
15. Mannella CA. Structure and dynamics of the mitochondrial inner membrane cristae. Biochim Biophys Acta. 2006; 1763:542–8. [PubMed: 16730811]
16. Mannella CA. Structural diversity of mitochondria: functional implications. Ann N Y Acad Sci. 2008; 1147:171–9. [PubMed: 19076440]
17. Scorrano L, Ashiya M, Buttle K, Weiler S, Oakes SA, Mannella CA, et al. A distinct pathway remodels mitochondrial cristae and mobilizes cytochrome c during apoptosis. Dev Cell. 2002; 2:55–67. [PubMed: 11782314]
18. Sun MG, Williams J, Munoz-Pinedo C, Perkins GA, Brown JM, Ellisman MH, et al. Correlated three-dimensional light and electron microscopy reveals transformation of mitochondria during apoptosis. Nat Cell Biol. 2007; 9:1057–65. [PubMed: 17721514]
19. van Driel LF, Valentijn JA, Valentijn KM, Koning RI, Koster AJ. Tools for correlative cryo-fluorescence microscopy and cryo-electron tomography applied to whole mitochondria in human endothelial cells. Eur J Cell Biol. 2009; 88:669–84. [PubMed: 19726102]
20. Nicastro D, Frangakis AS, Typke D, Baumeister W. Cryo-electron tomography of neurospora mitochondria. J Struct Biol. 2000; 129:48–56. [PubMed: 10675296]
21. Hsieh CE, Leith A, Mannella CA, Frank J, Marko M. Towards high-resolution three-dimensional imaging of native mammalian tissue: electron tomography of frozen-hydrated rat liver sections. J Struct Biol. 2006; 153:1–13. [PubMed: 16343943]
22. Amutha B, Gordon DM, Gu Y, Pain D. A novel role of Mgm1p, a dynamin-related GTPase, in ATP synthase assembly and cristae formation/maintenance. Biochem J. 2004; 381:19–23. [PubMed: 15125685]
23. Meeusen S, DeVay R, Block J, Cassidy-Stone A, Wayson S, McCaffery JM, et al. Mitochondrial inner-membrane fusion and crista maintenance requires the dynamin-related GTPase Mgm1. Cell. 2006; 127:383–95. [PubMed: 17055438]
24. Frezza C, Cipolat S, Martins de Brito O, Micaroni M, Beznoussenko GV, Rudka T, et al. OPA1 controls apoptotic cristae remodeling independently from mitochondrial fusion. Cell. 2006; 126:177–89. [PubMed: 16839885]
25. Agier V, Oliviero P, Laine J, L'Hermitte-Stead C, Girard S, Fillaut S, et al. Defective mitochondrial fusion, altered respiratory function, and distorted cristae structure in skin fibroblasts with heterozygous OPA1 mutations. Biochim Biophys Acta. 2012; 1822:1570–80. [PubMed: 22800932]
26. Kanazawa T, Zappaterra MD, Hasegawa A, Wright AP, Newman-Smith ED, Buttle KF, et al. The *C. elegans* Opa1 homologue EAT-3 is essential for resistance to free radicals. PLoS Genet. 2008; 4:e1000022. [PubMed: 18454199]
27. Zick M, Rabl R, Reichert AS. Cristae formation-linking ultrastructure and function of mitochondria. Biochim Biophys Acta. 2009; 1793:5–19. [PubMed: 18620004]
28. Allen RD, Schroeder CC, Fok AK. An investigation of mitochondrial inner membranes by rapid-freeze deep-etch techniques. J Cell Biol. 1989; 108:2233–40. [PubMed: 2525561]
29. Paumard P, Vaillier J, Coulary B, Schaeffer J, Soubannier V, Mueller DM, et al. The ATP synthase is involved in generating mitochondrial cristae morphology. EMBO J. 2002; 21:221–30. [PubMed: 11823415]
30. Minauro-Sanmiguel F, Wilkens S, Garcia JJ. Structure of dimeric mitochondrial ATP synthase: novel F0 bridging features and the structural basis of mitochondrial cristae biogenesis. Proc Natl Acad Sci U S A. 2005; 102:12356–8. [PubMed: 16105947]
31. Dudkina NV, Heinemeyer J, Keegstra W, Boekema EJ, Braun HP. Structure of dimeric ATP synthase from mitochondria: an angular association of monomers induces the strong curvature of the inner membrane. FEBS Lett. 2005; 579:5769–72. [PubMed: 16223490]

32. Davies KM, Anselmi C, Wittig I, Faraldo-Gomez JD, Kuhlbrandt W. Structure of the yeast F1Fo-ATP synthase dimer and its role in shaping the mitochondrial cristae. Proc Natl Acad Sci U S A. 2012; 109:13602–7. [PubMed: 22864911]
33. John GB, Shang Y, Li L, Renken C, Mannella CA, Selker JM, et al. The mitochondrial inner membrane protein mitofilin controls cristae morphology. Mol Biol Cell. 2005; 16:1543–54. [PubMed: 15647377]
34. Hoppins S, Collins SR, Cassidy-Stone A, Hummel E, Devay RM, Lackner LL, et al. A mitochondrial-focused genetic interaction map reveals a scaffold-like complex required for inner membrane organization in mitochondria. J Cell Biol. 2011; 195:323–40. [PubMed: 21987634]
35. Harner M, Korner C, Walther D, Mokranjac D, Kaesmacher J, Welsch U, et al. The mitochondrial contact site complex, a determinant of mitochondrial architecture. EMBO J. 2011; 30:4356–70. [PubMed: 22009199]
36. Darshi M, Mendiola VL, Mackey MR, Murphy AN, Koller A, Perkins GA, et al. ChChd3, an inner mitochondrial membrane protein, is essential for maintaining crista integrity and mitochondrial function. J Biol Chem. 2011; 286:2918–32. [PubMed: 21081504]
37. Zerbes RM, Bohnert M, Stroud DA, von der Malsburg K, Kram A, Oeljeklaus S, et al. Role of MINOS in mitochondrial membrane architecture: cristae morphology and outer membrane interactions differentially depend on mitofilin domains. J Mol Biol. 2012; 422:183–91. [PubMed: 22575891]
38. Dudkina NV, Oostergetel GT, Lewejohann D, Braun HP, Boekema EJ. Row-like organization of ATP synthase in intact mitochondria determined by cryo-electron tomography. Biochim Biophys Acta. 2010; 1797:272–7. [PubMed: 19925775]
39. Lenaz G, Genova ML. Structural and functional organization of the mitochondrial respiratory chain: a dynamic super-assembly. Int J Biochem Cell Biol. 2009; 41:1750–72. [PubMed: 19711505]
40. Gilkerson RW, Selker JM, Capaldi RA. The cristal membrane of mitochondria is the principal site of oxidative phosphorylation. FEBS Lett. 2003; 546:355–8. [PubMed: 12832068]
41. Vogel F, Bornhovd C, Neupert W, Reichert AS. Dynamic subcompartmentalization of the mitochondrial inner membrane. J Cell Biol. 2006; 175:237–47. [PubMed: 17043137]
42. Hoppel CL, Tandler B, Fujioka H, Riva A. Dynamic organization of mitochondria in human heart and in myocardial disease. Int J Biochem Cell Biol. 2009; 41:1949–56. [PubMed: 19446651]
43. Riva A, Tandler B, Loffredo F, Vazquez E, Hoppel C. Structural differences in two biochemically defined populations of cardiac mitochondria. Am J Physiol Heart Circ Physiol. 2005; 289:H868–72. [PubMed: 15821034]
44. Chikando AC, Kettlewell S, Williams GS, Smith G, Lederer WJ. Ca(2+) dynamics in the mitochondria — state of the art. J Mol Cell Cardiol. 2011; 51:627–31. [PubMed: 21864537]
45. Bertram R, Budu-Grajdeanu P, Jafri MS. Using phase relations to identify potential mechanisms for metabolic oscillations in isolated beta-cell mitochondria. Islets. 2009; 1:87–94. [PubMed: 21099254]
46. Nguyen MH, Dudycha SJ, Jafri MS. Effect of Ca2+ on cardiac mitochondrial energy production is modulated by Na+ and H+ dynamics. Am J Physiol Cell Physiol. 2007; 292:C2004–20. [PubMed: 17344315]
47. Dash RK, Qi F, Beard DA. A biophysically based mathematical model for the kinetics of mitochondrial calcium uniporter. Biophys J. 2009; 96:1318–32. [PubMed: 19217850]
48. Dash RK, Beard DA. Analysis of cardiac mitochondrial Na+ – Ca2+ exchanger kinetics with a biophysical model of mitochondrial Ca2+ handling suggests a 3:1 stoichiometry. J Physiol. 2008; 586:3267–85. [PubMed: 18467367]
49. Wei AC, Liu T, Winslow RL, O'Rourke B. Dynamics of matrix-free Ca2+ in cardiac mitochondria: two components of Ca2+ uptake and role of phosphate buffering. J Gen Physiol. 2012; 139:465–78. [PubMed: 22641641]
50. Habersetzer J, Ziani W, Larrieu I, Stines-Chaumeil C, Giraud MF, Brethes D, et al. ATP synthase oligomerization: from the enzyme models to the mitochondrial morphology. Int J Biochem Cell Biol. 2013; 45:99–105. [PubMed: 22664329]

51. Marko M, Hsieh C, Schalek R, Frank J, Mannella C. Focused-ion-beam thinning of frozen-hydrated biological specimens for cryo-electron microscopy. Nat Methods. 2007; 4:215–7. [PubMed: 17277781]

52. Brown TA, Tkachuk AN, Shtengel G, Kopek BG, Bogenhagen DF, Hess HF, et al. Superresolution fluorescence imaging of mitochondrial nucleoids reveals their spatial range, limits, and membrane interaction. Mol Cell Biol. 2011; 31:4994–5010. [PubMed: 22006021]

53. Chvanov M. Metabolic control of elastic properties of the inner mitochondrial membrane. J Phys Chem B. 2006; 110:22903–9. [PubMed: 17092042]

54. Muster B, Kohl W, Wittig I, Strecker V, Joos F, Haase W, et al. Respiratory chain complexes in dynamic mitochondria display a patchy distribution in life cells. PLoS One. 2010; 5:e11910. [PubMed: 20689601]

55. Shu X, Lev-Ram V, Deerinck TJ, Qi Y, Ramko EB, Davidson MW, et al. A genetically encoded tag for correlated light and electron microscopy of intact cells, tissues, and organisms. PLoS Biol. 2011; 9:e1001041. [PubMed: 21483721]

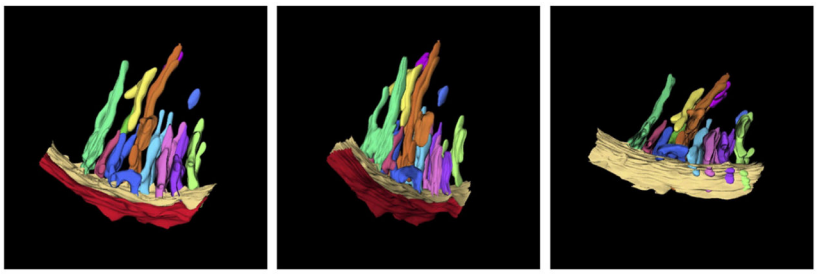

Fig. 1.

Three dimensional membrane structure of an avian cardiac muscle mitochondrion, obtained by electron tomography. The pleomorphic nature of the closely packed cristae is evident. The tilted view reveals the narrow openings of the cristae (crista junctions) into the boundary region of the inner membrane. The reconstructed sector of this mitochondrion is ca. 300 nm in length. Used with generous permission from Z. Almsherqi and Y. Deng.

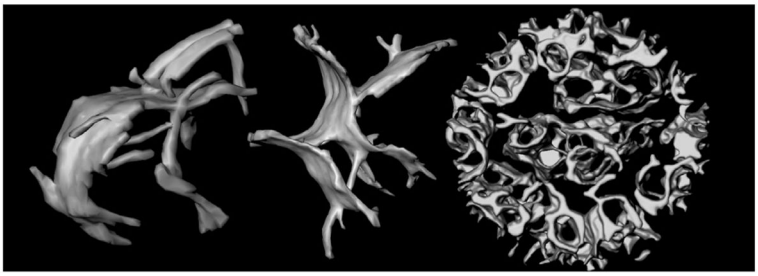

Fig. 2.

Topology of mitochondrial inner membranes. Left and middle: Cristae in intact, frozen-hydrated rat-liver mitochondria. The larger compartments appear to be formed by fusion of tubular membranes. These cristae are ca. 600 nm in length. Right: Inner membrane of a mouse liver mitochondrion after treatment with the pro-apoptotic protein t-Bid [17]. Curvature of the crista membranes is reversed and the intracristal space essentially forms one continuous compartment. The diameter of this mitochondrion is 860 nm. Figure from Mannella (2008), *Annals New York Acad Sci* [16] reproduced with permission of the publisher (Elsevier).

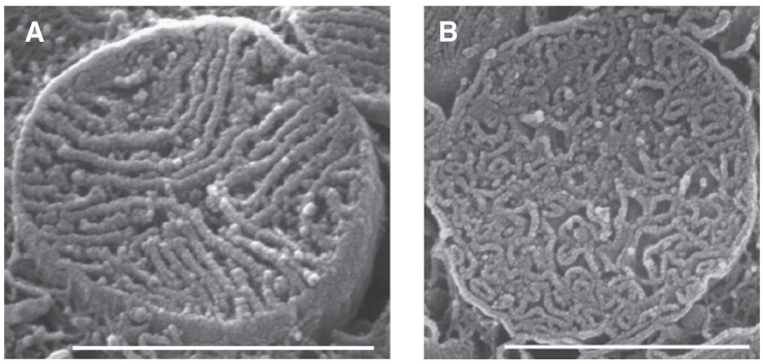

Fig. 3.

Densely packed cristae in cardiac ventricular myocytes. Scanning EM images of mitochondria cristae from rat ventricular myocytes. A. Lamellar cristae. B. Tubular cristae. Scale bars 1 — μm; cristae width are about 30 nm. Figure from Hoppel et al. (2009) *Int J Biochem Cell Biol* [42,43], reproduced with permission of the publisher (Elsevier).

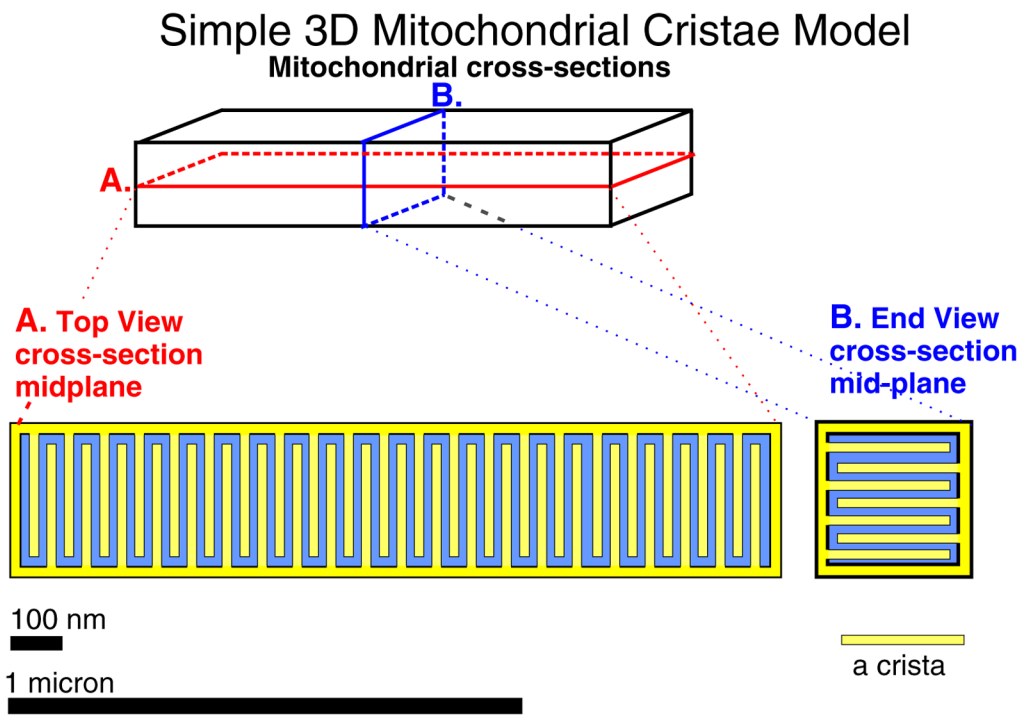

Fig. 4.

Simple mitochondrial cristae model in 3D. An intermyofibrillar mitochondrion (IFM) of size 1500 nm × 300 nm × 300 nm. A. Top view, cross-section, mid-plane. B. End view cross-section mid-plane. Each crista in the model is 240 nm long × 20 nm square and separated from other cristae by 20 nm. There are 42 cristae in a 40 nm plane and 7 layers of cristae, for a total of 294 cristae. The surface area per crista is 240 nm × 20 nm × 4 + 20 × 20 nm^2 or 1.96 10^4 nm^2. Thus the surface area of the inner membrane is 1.96 10^4 × 294 or 5.76 10^6 nm^2, which is about three times larger than the surface area of the outer member, 1.98 10^6 nm^2. The matrix is approximately half of the volume contained within the outer membrane. As noted, other shapes of the cristae may occur and will affect mitochondrial function.

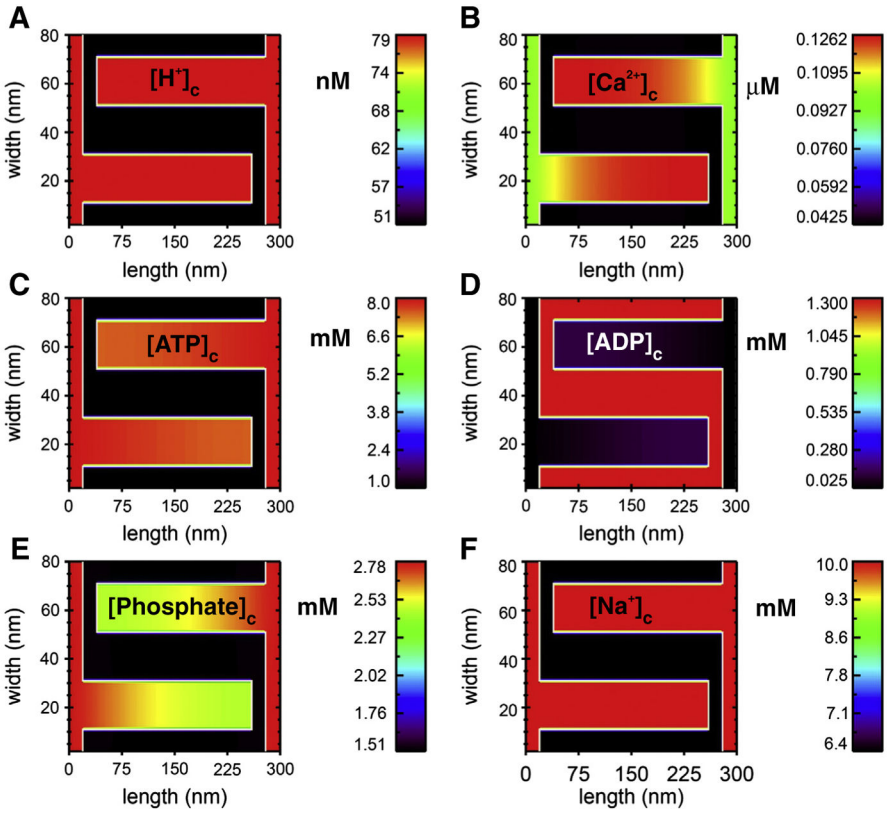

Fig. 5.

Diffusion down the length of cristae modeled as a 2D structure. Using a simple two-dimensional transport model (based on the study of Nguyen, Dudycha and Jafri in 2007 [46]) with the mitochondrial geometry of Fig. 4, steady-state crista gradients are shown for 6 solutes in a simulation run to steady state. This model includes the tricarboxylic acid, electron transport chain fluxes, ionic homeostasis (including H^+, Ca^{2+}, ATP, ADP, P_i and Na^+) and the adenine nucleotide translocase (ANT) among other features [46]. The fluxes are uniformly distributed along the mitochondrial inner membrane (white line in the figure), about 93% of which lies within the cristae in this model (about 78% in the model of Fig. 4). The behavior of these components was modeled after biochemical/biophysical measurements. The maximal fluxes of each of the component were constrained to give appropriate metabolite concentrations, total Krebs cycle fluxes, ATP production, membrane potential, and ionic homeostasis. The outer membrane is assumed to be permeable with respect to the modeled substances and was thus treated as a fixed boundary condition with cytosolic concentrations of metabolites. The sides of the two zoomed-in cristae are treated with periodic boundary conditions to mimic the repeated structures of the mitochondria (see Fig. 4). The images show the steady-state profiles (after 0.5 ms simulation time) of the six solutes under diastolic conditions. A. $[H^+]_c$ in nM. B. $[Ca^{2+}]_c$ in μM. C. $[ATP]_c$ in mM. D. $[ADP]_c$ in mM. E. $[Phosphate]_c$ in mM. F. $[Na^+]_c$ in mM. Initial conditions: The intermembrane space adjacent to the outer membrane at the ends of the cristae are assumed to have concentrations equal to the cytosol (i.e. the outer membrane is no permeability barrier for these substances).

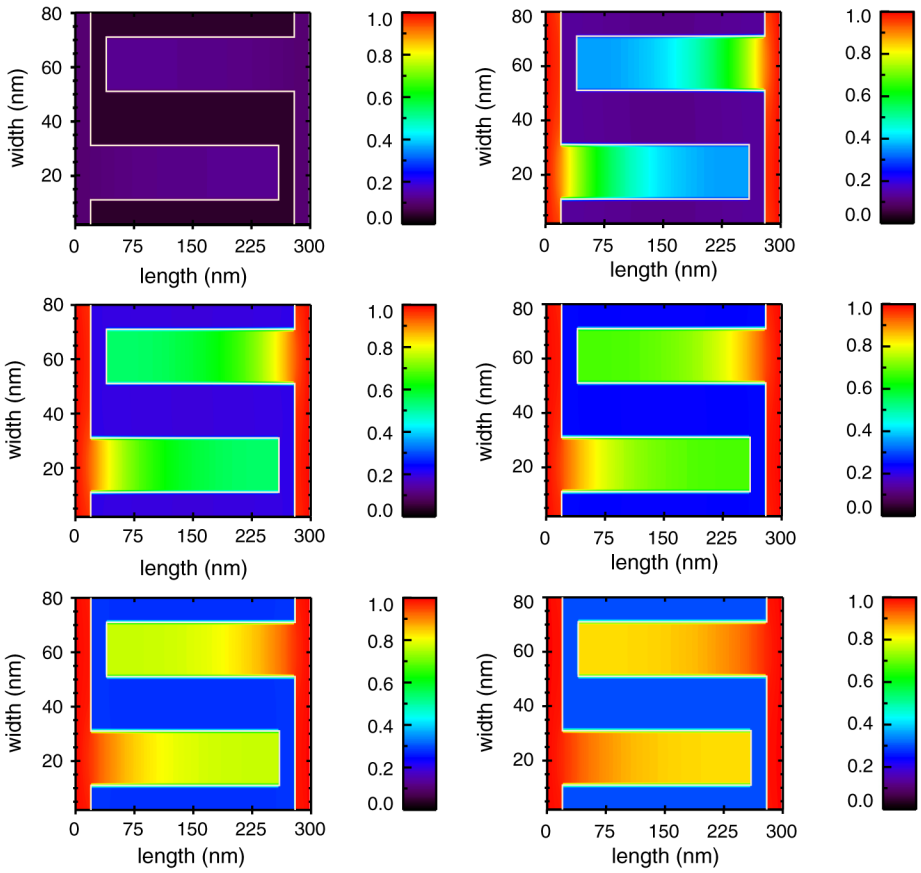

Fig. 6.

Time-course of cristae $[Ca^{2+}]$ ($[Ca^{2+}]_c$) following a 1 μM elevation of $[Ca^{2+}]_i$ from 100 nM. Using the same model as in Fig. 5 the time-course of an increase of $[Ca^{2+}]_c$ over 0.5 ms in five 0.1 ms steps. Upper left panel: before (0.0 ms, equal to the steady-state conditions from Fig. 5B); lower right panel: after 0.5 ms the diffusion of $[Ca^{2+}]_c$ has come to a new steady-state. An animation of this simulation is provided as a Supplemental Material.